Clarifications on the Damping Mechanism Related to the Hunting Motion of the Wheel Axle of a High-Speed Railway Vehicle

Barenten Suciu

Abstract—In order to explain the damping mechanism, related to the hunting motion of the wheel axle of a high-speed railway vehicle, a generalized dynamic model is proposed. Based on such model, analytic expressions for the damping coefficient and damped natural frequency are derived, without imposing restrictions on the ratio between the lateral and vertical creep coefficients. Influence of the travelling speed, wheel conicity, dimensionless mass of the wheel axle, ratio of the creep coefficients, ratio of the track span to the yawing diameter, etc. on the damping coefficient and damped natural frequency, is clarified.

Keywords—High-speed railway vehicle, hunting motion, wheel axle, damping, creep, vibration model, analysis.

I. INTRODUCTION

IN order to further increase the travelling speed of the bullet trains, a deeper understanding of the hunting motion is required. Among various vibration modes associated to the snake-like movement of the railway vehicle, the hunting motion of the wheel axle requires the simplest analysis. However, even in such relatively easy-to-understand study case, analytical expressions for the natural frequency of hunting were obtained only based on a geometrical model [1], [2]. Since such simplified model was developed under the assumption that the inertial effects, i.e. the mass of the wheel axle, can be neglected, the dynamical effects associated to the hunting motion were implicitly disregarded [3]. Moreover, the geometrical model is unable to predict the damping effect induced by the contact of the wheels with the rails [4], [5].

On one hand, in the absence of damping, under excitation, the mechanical system will continue to vibrate indefinitely [6], [7]. Thus, it appears that once started, the hunting vibration of the wheel axle cannot be naturally halted (attenuated). However, such result disagrees with the hunting behavior observed on actual railway carriages [1], [2]. On the other hand, although the creep phenomenon, occurring at the contact of the wheels with the rails, is well-known [8]-[13], the connection between the creep and the damping is still to be clarified.

Accordingly, in this work, the hunting vibration model is improved by introducing the inertial effects, by removing the geometrical constraints concerning the rotation of the wheel axle, and by relaxing the tribological restrictions on the ratio of the lateral and vertical creep coefficients. Specifically, explicit

Barenten Suciu is with the Department of Intelligent Mechanical Engineering, Fukuoka Institute of Technology, Fukuoka, 811-0295 Japan (phone: +81-92-606-4348; fax: +81-92-606-0747; e-mail: suciu@fit.ac.jp).

relations of calculus for the damping coefficient and damped natural frequency are derived, in the case of dynamical hunting motion. Then, the influence of the geometrical, kinematical, inertial and tribological parameters on the damping coefficient and damped natural frequency is emphasized.

II. MODEL ASSOCIATED TO THE HUNTING MOTION OF THE RAILWAY WHEEL AXLE

Following the basic idea, advanced by Leonardo da Vinci, of a mechanism using a double-cone that self-propels upwardly on straight divergent rails, in 1829 the applicative idea of a self-driven train was proposed [14]. Concept of such *gravitational locomotive* was abandoned, in competition with locomotives employing combustible and electrical energy sources. Still, nowadays, the wheel tread of the railway vehicles is slightly conical [1], [15]. Moreover, the whole wheel axle can be circumscribed by a double-cone, which has a total height of $2H$, a diameter at the conical base of $2R$, and an apex angle of $\Psi = \tan^{-1}(R/H)$ (see Fig. 1).
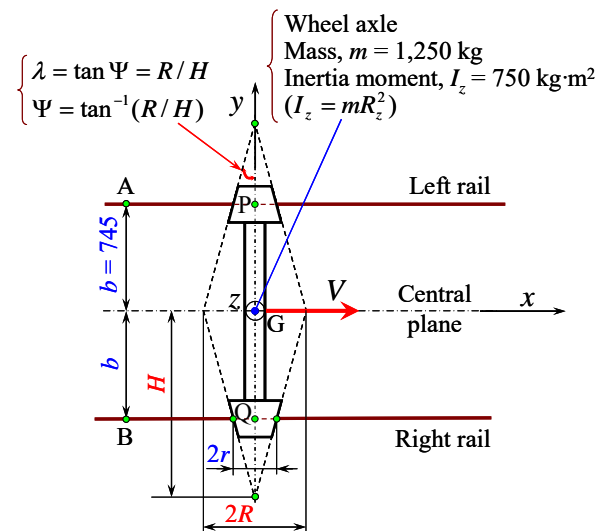

Fig. 1 Geometrical and inertial parameters of a wheel axle that travels with a velocity V on parallel rails, of span $2b$

Fig. 1 presents a wheel axle travelling with a velocity V on parallel rails, of span $2b$. G denotes the mass center of the wheel axle. P and Q are the contact points of the wheels with the left and right rails, respectively.

In order to describe the fundamental hunting motion, Fig. 2

World Academy of Science, Engineering and Technology
International Journal of Aerospace and Mechanical Engineering
Vol:12, No:1, 2018

shows the wheel axle under a small displacement perturbation δ, taken along the lateral axis y, and superposed on a small angular perturbation θ, taken around the vertical axis z. P' and Q' represent the contact points of the wheels with the rails, when the mass center shifts to the point G', under the lateral perturbation.
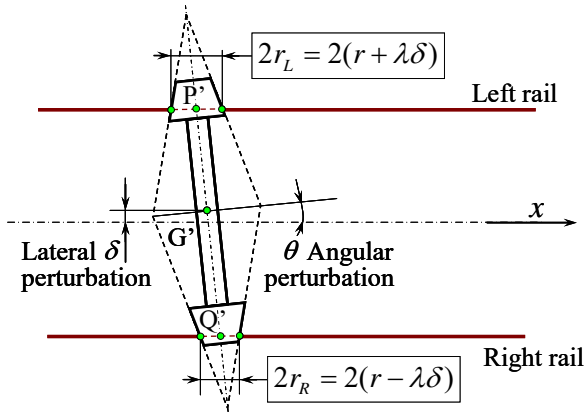

Fig. 2 Geometrical model for the contact of the wheel axle with the rails, during the hunting motion produced by lateral and angular perturbations

Under assumption that the lateral displacement δ is small, and also, the slope of the conical wheel tread $\lambda = \tan \Psi = R/H$ is small, the left radius of contact r_L corresponding to point P', and the right radius of contact r_R corresponding to point Q' can be calculated as [1], [2]:

$$r_L = r + \delta\lambda \geq r \quad ; \quad r_R = r - \delta\lambda \leq r \qquad (1)$$

where r is the contact radius of the unperturbed wheel axle.

Due to the conical geometry of the wheels, the contact radius at the left wheel increases, and at the right wheel decreases, this producing a wedge effect that opposes the perturbation.

Hunting vibration of the railway wheel axle can be described by the following set of two differential equations [1]-[3]:

$$\begin{cases} m\ddot{\delta} + \dfrac{f_2}{V}\dot{\delta} - f_2\theta = 0 \\[3mm] mR_z^2\ddot{\theta} + \dfrac{f_1 b^2}{V}\dot{\theta} + \dfrac{f_1 b\lambda}{r}\delta = 0 \end{cases} \qquad (2)$$

where m denotes the mass of the wheel axle (Fig. 1), $I_z = mR_z^2$ is the yawing moment of inertia, corresponding to a rotation of the wheel axle around the vertical z axis (Fig. 1), R_z is the yaw gyration radius, f_1 is the vertical creep coefficient, and f_2 is the horizontal or lateral creep coefficient (Fig. 3). The creep coefficients are taken for the whole wheel axle, i.e. they include the creep effects at both P' and Q' contact points.

Note that (2) was derived by assuming that displacements of the mass center along y and z axes, produced by the inclination

of the wheel axle, are small, and also, by supposing that the gyroscopic effects are negligible [1], [2]. For instance, if the displacements of the mass center along y and z axes, due to the inclination of the wheel axle, are to be considered, in (2) the terms containing the perturbation δ and the perturbation speed $\dot{\delta}$ should be corrected, by multiplying them with the quantity $1/(1 - r\lambda/b)$ [1]. However, the following dynamic analysis is done by accepting (2), as a sufficiently accurate starting point.

III. VIBRATION MODEL CORRESPONDING TO THE GEOMETRICAL HUNTING MODE

So-called *geometrical hunting mode* [1]-[3], is defined under the assumption that the inertial terms, of translation movement $m\ddot{\delta}$, and rotation movement $mR_z^2\ddot{\theta}$, can be neglected in (2). In the other words, supposing that the mass of the wheel axle can be neglected ($m \cong 0$), further simplification of (2) is achieved, as follows:

$$\begin{cases} \dfrac{f_2}{V}\dot{\delta} - f_2\theta = 0 \\[3mm] \dfrac{f_1 b^2}{V}\dot{\theta} + \dfrac{f_1 b\lambda}{r}\delta = 0 \end{cases} \qquad (3)$$

By applying a Laplace transformation to the set of equations (3), under nil initial conditions, and by substituting the coupling terms corresponding to the angle θ and the lateral perturbation δ from one equation to the other, the following characteristic equation can be derived [1]-[3]:

$$s^2 + \frac{\lambda V^2}{rb} = 0 \qquad (4)$$

Next, by rewriting Laplace operator as $s = i\omega_g$, the natural circular frequency, corresponding to the geometrical hunting motion can be obtained as [3]:

$$\omega_g = V\sqrt{\frac{\lambda}{rb}} \qquad (5)$$

Usually, (5) is rewritten as follows, to obtain the well-known wavelength of the geometrical hunting motion [1]-[3]:

$$S_g = V \cdot T_g = \frac{V}{f_g} = 2\pi\frac{V}{\omega_g} = 2\pi\sqrt{\frac{rb}{\lambda}} \qquad (6)$$

where T_g is the period, and f_g is the natural frequency of the geometrical hunting mode.

In conclusion, under the relative drastic simplification of the vibration model, i.e. under the assumption that the mass of the wheel axle can be neglected, an explicit relation for the circular frequency of the hunting mode was achieved. However, since (4) does not contain a term in s, it appears that the mechanical

World Academy of Science, Engineering and Technology
International Journal of Aerospace and Mechanical Engineering
Vol:12, No:1, 2018

system is undamped. Thus, once excited, the hunting vibration of the wheel axle cannot be naturally halted (attenuated), this being a result in disagreement with the hunting behavior observed on the actual railway vehicles [1], [2]. For this reason, improvement of the vibration model is required.

IV. VIBRATION MODEL CORRESPONDING TO THE INERTIAL OR DYNAMICAL HUNTING MODE

If the inertia terms $m\ddot{\delta}$ and $mR_z^2\ddot{\theta}$ are not neglected in (2), after performing the Laplace transformation of the equations of movement, the characteristic equation of the system can be written as [1]-[3]:

$$s^4 + \frac{f_1 b^2 + f_2 R_z^2}{mR_z^2 V}s^3 + \frac{f_1 f_2 b^2}{m^2 R_z^2 V^2}s^2 + \frac{f_1 f_2 b\lambda}{m^2 R_z^2 r} = 0 \qquad (7)$$

Thus, (7) appears as a fourth order polynomial equation, having a missing term, which corresponds to s:

$$A_0 s^4 + A_1 s^3 + A_2 s^2 + A_3 = 0 \qquad (8)$$

where the polynomial coefficients can be identified as follows:

$$\begin{cases} A_0 = 1 \\ \\ A_1 = \dfrac{f_1 b^2 + f_2 R_z^2}{mR_z^2 V} = \omega_c(\bar{b}^2 + \bar{f}) \\ \\ A_2 = \dfrac{f_1 f_2 b^2}{m^2 R_z^2 V^2} = \omega_c^2 \bar{b}^2 \bar{f} \\ \\ A_3 = \dfrac{f_1 f_2 b\lambda}{m^2 R_z^2 r} = \omega_c^2 \omega_g^2 \bar{b}^2 \bar{f} \end{cases} \qquad (9)$$

Thus, the polynomial coefficients (9) are depending on the *creep circular frequency* ω_c, on the *creep ratio* $\bar{f}$ (i.e., ratio of the lateral creep coefficient to the vertical creep coefficient), as well as on the *dimensionless contact width* $\bar{b}$ (i.e., ratio of the track span $2b$ to the yawing diameter $2R_z$ of gyration). These dependence parameters can be calculated as follows:

$$\omega_c = f_1/(mV) \quad ; \quad \bar{f} = f_2/f_1 \quad ; \quad \bar{b} = b/R_z \qquad (10)$$

Both theoretical [8], [10] and experimental [11] evaluations of the vertical and lateral creep coefficients can be found in the literature. Accordingly, a variation range of $\bar{f} = 0.8 - 0.97$ can be accepted for the creep ratio (see Table I). However, in order to simplify the analysis of the hunting motion, it is customarily considered that the lateral creep coefficient almost equals the vertical creep coefficient, and consequently, $\bar{f} \cong 1$ [1]-[5]. On the other hand, dimensionless contact width is close to one ($\bar{b} \cong 1$), for various types of railway carriages. For instance, in

the case of the Japanese bullet trains, *Shinkansen*, since the semi-span of the rails is $b = 745$ mm, and the yaw gyration radius is about of $R_z = \sqrt{I_z/m} = 775$ mm, the dimensionless contact width displays a value of $\bar{b} = 0.96 \cong 1$ (see Table I).
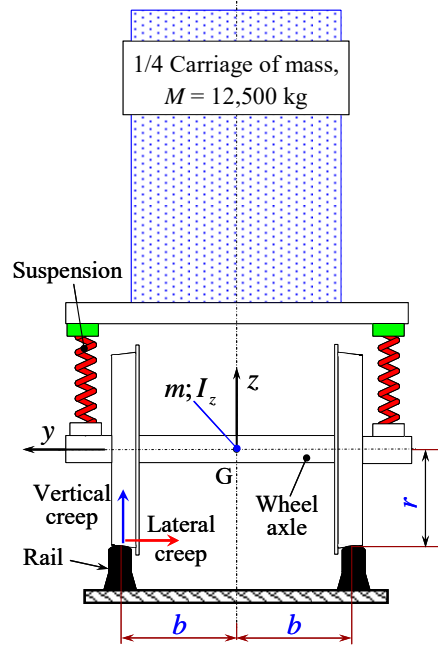

Fig. 3 Schematic view of one-quarter carriage, suspended on the wheel axle, as well as the vertical and lateral creep, occurring at the contact of the wheels with the rails

TABLE I
GEOMETRICAL AND PHYSICAL PROPERTIES OF THE WHEEL AXLE, RAILS AND RAILWAY CARRIAGE

Property	Value
Mass of one-quarter carriage, M [kg]	12,500 [16]
Mass of the wheel axle, m [kg]	1,250 [16]
Yawing inertia moment of the wheel axle, $I_z = mR_z^2$ [kg·m²]	750 [16]
Yawing inertia radius of the wheel axle, R_z [mm]	775 [17]
Wheel diameter, $2r$ [mm]	860 [3]
Wheel conicity, λ [-]	0; 0.01; 0.025; 0.05; 0.1; 0.2 [15]
Rails span, b [mm]	745 [3]
Dimensionless contact width, $\bar{b} = b/R_z$ [-]	0.96 [17]
Creep ratio, $\bar{f} = f_2/f_1$ [-]	0.8 – 0.97 [8], [10], [11]

Such tribological and geometrical restrictions ($\bar{b} \cong \bar{f} \cong 1$) are not mandatory in the case of the present approach of the hunting vibration. Thus, the proposed model leads to explicit expressions for the damping coefficients and for the damped circular frequency, under a generalized approach of the wheel axle hunting motion.

Next, the following change of variable is applied to (8):

$$s = S - A_1/4 \qquad (11)$$

World Academy of Science, Engineering and Technology
International Journal of Aerospace and Mechanical Engineering
Vol:12, No:1, 2018

Under this new variable S, the characteristic equation can be rewritten as:

$$S^4 + B_1 S^2 + B_2 S + B_3 = 0 \qquad (12)$$

where the polynomial coefficients attached to (12) are given by:

$$B_1 = A_2 - \frac{3}{8} A_1^2 = -\frac{\omega_c^2}{8} [2(\bar{b}^4 + \bar{f}^2) + (\bar{b}^2 - \bar{f})^2] \cong$$
$$\cong -\frac{\omega_c^2}{4}(\bar{b}^4 + \bar{f}^2) \qquad (13)$$

$$B_2 = \frac{1}{2} A_1 (\frac{A_1^2}{4} - A_2) = \frac{\omega_c^3}{8}(\bar{b}^2 + \bar{f}) \cdot (\bar{b}^2 - \bar{f})^2 \cong 0 \qquad (14)$$

$$B_3 = A_3 + \frac{A_2 A_1^2}{16} - \frac{3A_1^4}{256} = \frac{\omega_c^4}{256}[256(\frac{\omega_g}{\omega_c})^2 \bar{b}^2 \bar{f} +$$
$$+ 16\bar{b}^2 \bar{f}(\bar{b}^2 + \bar{f})^2 - 3(\bar{b}^2 + \bar{f})^4] \qquad (15)$$

Since the maximal value of the term $(\bar{b}^2 - \bar{f})^2$, occurring in (13) and (14), can be estimated as:

$$(\bar{b}^2 - \bar{f})^2_{\max} = (0.96^2 - 0.8)^2 = 0.015 << 1 \qquad (16)$$

one concludes that it can be neglected ($(\bar{b}^2 - \bar{f})^2 \cong 0$). Hence, the severer restriction $\bar{b} \cong \bar{f} \cong 1$, usually used in the study of the hunting motion, can be replaced by a milder restriction ($(\bar{b}^2 - \bar{f})^2 \cong 0$), to fulfill the analysis. As an advantage of such approach, the influence of the creep ratio, and the influence of the dimensionless contact width, on the damped frequency, and on the damping ratio, can be clarified. Moreover, since $B_2 \cong 0$, the characteristic equation can be analytically solved, by rewriting it, as follows:

$$\sigma^2 + B_1 \sigma + B_3 = 0 \quad ; \quad \sigma = S^2 \qquad (17)$$

Thus, the discriminant of (17) can be calculated as:

$$\Delta = B_1^2 - 4B_3 = \omega_c^4 \{ \frac{(\bar{b}^2 - \bar{f})^2}{16}[(\bar{b}^2 + \bar{f})^2 + 2(\bar{b}^4 + \bar{f}^2)] -$$
$$- 4(\frac{\omega_g}{\omega_c})^2 \bar{b}^2 \bar{f} \} \cong -4\omega_c^2 \omega_g^2 \bar{b}^2 \bar{f} = 4i^2 \omega_c^2 \omega_g^2 \bar{b}^2 \bar{f} \qquad (18)$$

and then, the solutions of (17) can be expressed as follows:

$$\sigma_{1,2} = \frac{-B_1 \pm \sqrt{\Delta}}{2} = \frac{\omega_c^2}{8}(\bar{b}^4 + \bar{f}^2) \pm i\omega_c \omega_g \bar{b}\sqrt{\bar{f}} \qquad (19)$$

Note that, by taking in (19) the dimensionless contact width and the creep ratio as $\bar{b} \cong \bar{f} \cong 1$, solutions of the characteristic equation reduce to the following form:

$$\sigma_{1,2} \cong \frac{\omega_c^2}{4} \pm i\omega_c \omega_g \qquad (20)$$

a result which agrees with findings reported by [3].

Next, by employing (19), (17), and (11), one reverses the change of variables, from σ to S, and then, from S to s, and obtains all the four solutions of the characteristic equation, as listed below:

$$s_1 = S_1 - \frac{A_1}{4} = \sqrt{\sigma_1} - \frac{\omega_c}{4}(\bar{b}^2 + \bar{f}) =$$
$$= -\frac{\omega_c}{4}(\bar{b}^2 + \bar{f}) + \frac{\omega_c}{2}\sqrt{\frac{\bar{b}^4 + \bar{f}^2}{2} + 4i\frac{\omega_g}{\omega_c}\bar{b}\sqrt{\bar{f}}} \qquad (21)$$

$$s_2 = S_2 - \frac{A_1}{4} = -\sqrt{\sigma_1} - \frac{\omega_c}{4}(\bar{b}^2 + \bar{f}) =$$
$$= -\frac{\omega_c}{4}(\bar{b}^2 + \bar{f}) - \frac{\omega_c}{2}\sqrt{\frac{\bar{b}^4 + \bar{f}^2}{2} + 4i\frac{\omega_g}{\omega_c}\bar{b}\sqrt{\bar{f}}} \qquad (22)$$

$$s_3 = S_3 - \frac{A_1}{4} = \sqrt{\sigma_2} - \frac{\omega_c}{4}(\bar{b}^2 + \bar{f}) =$$
$$= -\frac{\omega_c}{4}(\bar{b}^2 + \bar{f}) + \frac{\omega_c}{2}\sqrt{\frac{\bar{b}^4 + \bar{f}^2}{2} - 4i\frac{\omega_g}{\omega_c}\bar{b}\sqrt{\bar{f}}} \qquad (23)$$

$$s_4 = S_4 - \frac{A_1}{4} = -\sqrt{\sigma_2} - \frac{\omega_c}{4}(\bar{b}^2 + \bar{f}) =$$
$$= -\frac{\omega_c}{4}(\bar{b}^2 + \bar{f}) - \frac{\omega_c}{2}\sqrt{\frac{\bar{b}^4 + \bar{f}^2}{2} - 4i\frac{\omega_g}{\omega_c}\bar{b}\sqrt{\bar{f}}} \qquad (24)$$

Then, it is useful to observe that the square roots occurring in (21)-(24), can be rewritten as:

$$\sqrt{\frac{\bar{b}^4 + \bar{f}^2}{2} \pm 4i\frac{\omega_g}{\omega_c}\bar{b}\sqrt{\bar{f}}} =$$
$$= \frac{\sqrt{\bar{b}^4 + \bar{f}^2}}{2}\left(\sqrt{\sqrt{1+\Sigma}+1} \pm i\sqrt{\sqrt{1+\Sigma}-1}\right) \qquad (25)$$

where Σ is a dimensionless parameter, which can be calculated as:

$$\Sigma = 64(\frac{\omega_g}{\omega_c})^2 \frac{\bar{b}^2 \bar{f}}{(\bar{b}^4 + \bar{f}^2)^2} \qquad (26)$$

Accordingly, (21)-(24) can be rewritten as:

$$s_1 = -\frac{\omega_c}{4}[(\bar{b}^2 + \bar{f}) - \sqrt{\bar{b}^4 + \bar{f}^2}\sqrt{\sqrt{1+\Sigma}+1}] +$$
$$+ i\frac{\omega_c}{4}\sqrt{\bar{b}^4 + \bar{f}^2}\sqrt{\sqrt{1+\Sigma}-1} \qquad (27)$$

World Academy of Science, Engineering and Technology
International Journal of Aerospace and Mechanical Engineering
Vol:12, No:1, 2018

$$s_2 = -\frac{\omega_c}{4}[(\bar{b}^2 + \bar{f}) + \sqrt{\bar{b}^4 + \bar{f}^2}\sqrt{\sqrt{1+\Sigma}+1}] -$$
$$- i\frac{\omega_c}{4}\sqrt{\bar{b}^4 + \bar{f}^2}\sqrt{\sqrt{1+\Sigma}-1} \tag{28}$$

$$s_3 = -\frac{\omega_c}{4}[(\bar{b}^2 + \bar{f}) - \sqrt{\bar{b}^4 + \bar{f}^2}\sqrt{\sqrt{1+\Sigma}+1}] -$$
$$- i\frac{\omega_c}{4}\sqrt{\bar{b}^4 + \bar{f}^2}\sqrt{\sqrt{1+\Sigma}-1} \tag{29}$$

$$s_4 = -\frac{\omega_c}{4}[(\bar{b}^2 + \bar{f}) + \sqrt{\bar{b}^4 + \bar{f}^2}\sqrt{\sqrt{1+\Sigma}+1}] +$$
$$+ i\frac{\omega_c}{4}\sqrt{\bar{b}^4 + \bar{f}^2}\sqrt{\sqrt{1+\Sigma}-1} \tag{30}$$

In order to identify the damping spontaneously occurring at the contact between the conical wheels and the rails, during the hunting motion of the railway wheel axle, one pays attention to similarities between (27)-(30), and solutions (31):

$$s_{5,6} = -\zeta\omega_n \pm i\omega_n\sqrt{1-\zeta^2} \tag{31}$$

which correspond to (32), i.e. to the characteristic equation of a classical damped one-degree of freedom vibration system, consisted of a spring connected in parallel to a dashpot [6], [7]:

$$s^2 + 2\zeta\omega_n s + \omega_n^2 = 0 \tag{32}$$

Here, ω_n is the natural circular frequency, and ζ is damping ratio, which has to satisfy the condition $0 < \zeta < 1$, in order to achieve damped oscillations [7].

Firstly, one observes that solutions s_1 and s_3 of (27) and (29), are similar to solutions s_5 and s_6 of (31). Corresponding natural circular frequency $\omega_{n,1}$ and damping ratio ζ_1 can be identified as follows:

$$\begin{cases} -\zeta_1\omega_{n,1} = -\frac{\omega_c}{4}[(\bar{b}^2 + \bar{f}) - \sqrt{\bar{b}^4 + \bar{f}^2}\sqrt{\sqrt{1+\Sigma}+1}] \\ \omega_{n,1}\sqrt{1-\zeta_1^2} = \frac{\omega_c}{4}\sqrt{\bar{b}^4 + \bar{f}^2}\sqrt{\sqrt{1+\Sigma}-1} \end{cases} \tag{33}$$

On the other hand, solutions s_2 and s_4 of (28) and (30), are similar to solutions s_5 and s_6 of (31). Again, corresponding natural circular frequency $\omega_{n,2}$ and damping ratio ζ_2 can be identified as:

$$\begin{cases} -\zeta_2\omega_{n,2} = -\frac{\omega_c}{4}[(\bar{b}^2 + \bar{f}) + \sqrt{\bar{b}^4 + \bar{f}^2}\sqrt{\sqrt{1+\Sigma}+1}] \\ \omega_{n,2}\sqrt{1-\zeta_2^2} = \frac{\omega_c}{4}\sqrt{\bar{b}^4 + \bar{f}^2}\sqrt{\sqrt{1+\Sigma}-1} \end{cases} \tag{34}$$

Looking to the lower parts of (33) and (34), one observes that the damped natural circular frequency ω_d, with respect to all the solutions s_1, s_2, s_3, s_4, displays the same value:

$$\omega_d = \omega_{n,1}\sqrt{1-\zeta_1^2} = \omega_{n,2}\sqrt{1-\zeta_2^2} =$$
$$= \frac{\omega_c}{4}\sqrt{\bar{b}^4 + \bar{f}^2}\sqrt{\sqrt{1+\Sigma}-1} =$$
$$= \frac{\omega_c}{4}\sqrt{(\bar{b}^2 - \bar{f})^2 + 2\bar{b}^2\bar{f}}\sqrt{\sqrt{1+\Sigma}-1}$$
$$\Downarrow$$
$$\omega_d \cong \frac{\sqrt{2}}{4}\omega_c\bar{b}\sqrt{\bar{f}}\sqrt{\sqrt{1+\Sigma}-1} \tag{35}$$

Then, from upper part of (34), one observes that regardless the values of parameters $\bar{b}$ and $\bar{f}$, the term $-\zeta_2\omega_{n,2} < 0$ displays a negative value. In conclusion, solutions s_2 and s_4 of the characteristic equation lead to a stable hunting movement, with a corresponding positive value for the damping coefficient ζ_2. On the other hand, regarding the upper part of (33), since the following inequality takes place:

$$(\bar{b}^2 + \bar{f}) < \sqrt{\bar{b}^4 + \bar{f}^2}\sqrt{\sqrt{1+\Sigma}+1}$$
$$\Downarrow$$
$$(\bar{b}^2 + \bar{f})^2 < (\bar{b}^4 + \bar{f}^2)(\sqrt{1+\Sigma}+1) \tag{36}$$
$$\Downarrow$$
$$2\bar{b}^2\bar{f}(1-\sqrt{1+\Sigma}) < 0$$

one concludes that regardless the values of parameters $\bar{b}$ and $\bar{f}$, the term $-\zeta_1\omega_{n,1} > 0$ shows a positive value. Consequently, solutions s_1 and s_3 of the characteristic equation lead to an unstable hunting motion, with a corresponding negative value for the damping coefficient ζ_1.

Solving (33)-(34) for the damping ratios of the inertial hunting, after some manipulations, the following analytical expressions for the damping ratios ζ_1 and ζ_2 can be obtained:

$$\begin{cases} \zeta_1 = -\sqrt{\frac{1}{2} - \frac{1}{2}\sqrt{\frac{2}{\sqrt{1+\Sigma}+1}}} < 0 \\ \zeta_2 = \sqrt{\frac{1}{2} + \frac{1}{2}\sqrt{\frac{2}{\sqrt{1+\Sigma}+1}}} > 0 \end{cases} \tag{37}$$

From (37), one notices that the damping ratios satisfy the following inequalities:

$$|\zeta_1| < \zeta_2 \quad \Rightarrow \quad \frac{\sqrt{1-\zeta_1^2}}{\sqrt{1-\zeta_2^2}} > 1 \tag{38}$$

World Academy of Science, Engineering and Technology
International Journal of Aerospace and Mechanical Engineering
Vol:12, No:1, 2018

which combined with (35), leads to the conclusion that the natural circular frequency $\omega_{n,1}$ is smaller than the natural circular frequency $\omega_{n,2}$:

$$\frac{\omega_{n,2}}{\omega_{n,1}} = \frac{\sqrt{1-\zeta_1^2}}{\sqrt{1-\zeta_2^2}} > 1 \qquad (39)$$

Summarizing, the natural circular frequency $\omega_{n,2}$ and the damping ratio ζ_2, corresponding to solutions s_2 and s_4 of the characteristic equation are larger than the natural circular frequency $\omega_{n,1}$ and the absolute value of the damping ratio $|\zeta_1|$ corresponding to solutions s_1 and s_3 of the characteristic equation (i.e., $\omega_{n,1} < \omega_{n,2}; |\zeta_1| < \zeta_2$). However, both hunting modes display the same value of the damped natural circular frequency ω_d.

Concerning the stability aspects of the hunting motion, it is possible to imagine that vibration δ_1 corresponding to solutions s_1 and s_3, as well as vibration δ_2 corresponding to solutions s_2 and s_4, satisfy the following equations of movement:

$$\begin{cases} \ddot{\delta}_1 + 2\zeta_1\omega_{n,1}\dot{\delta}_1 + \omega_{n,1}^2\delta_1 = 0 \\ \ddot{\delta}_2 + 2\zeta_2\omega_{n,2}\dot{\delta}_2 + \omega_{n,2}^2\delta_2 = 0 \end{cases} \qquad (40)$$

Solving the above set of differential equations, the following solutions for the vibrations δ_1 and δ_2 are obtained [6], [7]:

$$\begin{cases} \delta_1 = C_1\exp(-\zeta_1\omega_{n,1}t)\cos(\omega_d t - \Phi_1) \\ \delta_2 = C_2\exp(-\zeta_2\omega_{n,2}t)\cos(\omega_d t - \Phi_2) \end{cases} \qquad (41)$$

where C_1, C_2 are arbitrary constants, and Φ_1, Φ_2 are the initial phase angles. Since damping ratio ζ_2 is positive, as the time t elapses, the amplitude of vibration $C_2\exp(-\zeta_2\omega_{n,2}t)$ decreases, and this mode corresponds to a stable hunting motion. On the other hand, since the damping ratio ζ_1 is negative, as the time t elapses, the amplitude of vibration $C_1\exp(-\zeta_1\omega_{n,1}t)$ increases, and this mode corresponds to an unstable hunting motion.

V. RESULTS AND DISCUSSIONS

Summarizing the results concerning the hunting frequency, (5) defines the natural circular frequency ω_g, corresponding to the geometrical hunting motion, (10) defines an equivalent circular frequency ω_c, related to the creep phenomenon, and (35) defines the damped natural circular frequency ω_d,

corresponding to the inertial or dynamical hunting motion:

$$\begin{cases} \omega_g = V\sqrt{\dfrac{\lambda}{rb}} \quad ; \quad \omega_c = \dfrac{f_1}{mV} \\ \omega_d = \dfrac{\sqrt{2}}{4}\omega_c\bar{b}\sqrt{\bar{f}}\sqrt{\sqrt{1+\Sigma}-1} \end{cases} \qquad (42)$$

Dimensionless parameter Σ, introduced via (26), considerably influences the damped natural frequency and the damping ratio of the inertial hunting vibration. Further attention paid to Σ reveals that it can be calculated as (see (26)):

$$\Sigma \cong \frac{16}{b^2\bar{f}}\left(\frac{\omega_g}{\omega_c}\right)^2 = \frac{16}{b^2\bar{f}}\frac{m^2V^4\lambda}{f_1^2 rb} = \frac{16}{b^2\bar{f}}\frac{m^2V^4\lambda}{Mc^2r^2b} \qquad (43)$$

where in the above equation, the vertical creep coefficient f_1 was substituted as follows [8]:

$$f_1 = c\sqrt{rM} \text{ [N]}; \quad c = 2\times10^5 \text{ [(m×kg)}^{1/2}/\text{s}^2] \qquad (44)$$

In (44), the wheel radius can be taken as $r = 0.43\,\text{m}$, and the mass responsible for the creep phenomenon can be taken as one quarter of the total mass of the vehicle, i.e., as $M = 12,500\,\text{kg}$ (see Fig. 3 and Table I). In the end, the parameter Σ can be calculated as:

$$\Sigma = 32\pi\frac{\lambda\rho_e\bar{m}}{b^2\bar{f}c^2}V^4 \qquad (45)$$

where the parameters related to (45) are given by:

$$\bar{m} = \frac{m}{M} \quad ; \quad \rho_e = \frac{m}{V_e} \quad ; \quad V_e = (\pi r^2)\times(2b) \qquad (46)$$

Thus, (45)-(46) illustrate that the dimensionless parameter Σ proportionally depends on the fourth power of the travelling velocity of the railway vehicle, on the dimensionless mass $\bar{m}$ of the wheel axle (i.e., ratio of the mass m of the wheel axle to the mass M of one-quarter vehicle), on the slope λ of the wheel tread, and on the equivalent density ρ_e of the wheel axle (i.e., ratio of the mass m of the wheel axle to the volume V_e of the cylinder circumscribing the wheel axle). On the other hand, dimensionless parameter Σ depends inversely proportionally on the creep ratio $\bar{f}$ (i.e., ratio of the lateral creep coefficient to the vertical creep coefficient), on the second power of the dimensionless contact width $\bar{b}$ (i.e., ratio of the track span $2b$ to the yaw diameter $2R_z$ of gyration), and on the second power of the creep constant c.

Next, substituting into (42) the relationship between circular frequency ω_c, corresponding to the creep phenomenon, and the natural circular frequency ω_g, related to the geometrical

World Academy of Science, Engineering and Technology
International Journal of Aerospace and Mechanical Engineering
Vol:12, No:1, 2018

hunting motion:

$$\omega_c = 4\omega_g / (\bar{b}\sqrt{\bar{f}\cdot\Sigma}) \qquad (47)$$

one obtains the relationship between the natural circular frequencies, corresponding to the inertial, and geometrical hunting motions, as follows:

$$\omega_d = \omega_g \sqrt{\frac{2}{\sqrt{1+\Sigma}+1}} \leq \omega_g \qquad (48)$$

In conclusion, the damped natural circular frequency corresponding to the dynamical hunting motion is smaller than the natural circular frequency corresponding to the geometrical hunting motion (see Fig. 4). Only when the dimensionless parameter Σ is nil ($\Sigma = 0$), the inertial hunting frequency equals the geometrical hunting frequency ($\omega_d = \omega_g$). On one hand, $\Sigma = 0$ is obtained when the railway vehicle is at rest ($V = 0$), but in such case, the hunting motion is meaningless. On the other hand, $\Sigma = 0$ is obtained when the slope of the wheel tread is nil ($\lambda = 0$), i.e. the conical tread becomes cylindrical.

Next, one determines the values of the geometrical and dynamical hunting frequencies, in the case of a halted railway vehicle ($V = 0$), and in the case of a railway carriage running at very high speed ($V \to \infty$), as follows:

$$\begin{cases} \lim_{V\to 0}\omega_g = 0 \quad ; \quad \lim_{V\to\infty}\omega_g = \infty \\[2mm] \lim_{V\to 0}\omega_d = 0 \quad ; \quad \lim_{V\to\infty}\omega_d = \sqrt[4]{\dfrac{\lambda c^2 \bar{b}^2 \bar{f}}{4\bar{m}^2 bM}} \end{cases} \qquad (49)$$

Thus, the circular frequency corresponding to the geometrical hunting motion, linearly increases against the traveling speed, and tends to infinity for $V \to \infty$ (see Fig. 4). On the other hand, the damped natural circular frequency corresponding to the inertial hunting motion, non-linearly increases versus the travelling speed, but tends to a finite value when the railway vehicle is running at very high-speeds ($V \to \infty$) (see Fig. 4).

Concerning the damping ratio associated to the hunting motion, (37) combined with (45) illustrates that dissipation of the hunting vibration can be explained by the damping effect produced via creeping at the contact between rails and wheels.

Next, based on (37), one determines the values of the damping ratios ζ_1 and ζ_2, in the case of a halted railway vehicle ($V = 0$), and in the case of a railway carriage running at very high speed ($V \to \infty$), as follows:

$$\begin{cases} \lim_{V\to 0}\zeta_1 = 0 \quad ; \quad \lim_{V\to\infty}\zeta_1 = -\dfrac{\sqrt{2}}{2} \\[3mm] \lim_{V\to 0}\zeta_2 = 1 \quad ; \quad \lim_{V\to\infty}\zeta_2 = \dfrac{\sqrt{2}}{2} \end{cases} \qquad (50)$$
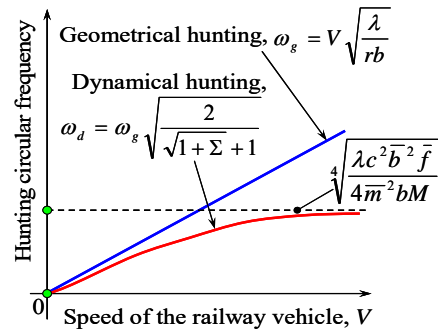

Fig. 4 Variation of the hunting circular frequency versus the travelling speed of the railway vehicle, in the case of the geometrical hunting mode, and in the case of the inertial (dynamical) hunting mode

Note that, both damping ratios ζ_1 and ζ_2 monotonically decrease at augmentation of the travelling speed of the railway vehicle (see Fig. 5).

For cylindrical wheels ($\lambda = 0$), the dimensionless parameter Σ is nil ($\Sigma = 0$), and in such conditions $\zeta_1 = 0$ and $\zeta_2 = 1$, regardless the travelling velocity of the vehicle.

In the absence of creep ($c = 0$), the dimensionless parameter Σ tends to infinity ($\Sigma \to \infty$), and in such circumstances $\zeta_1 = -\sqrt{2}/2$ and $\zeta_2 = \sqrt{2}/2$, regardless the travelling speed of the carriage.

It seems that in the absence of creep ($c = 0$), and also at very high travelling velocities of the railway vehicle ($V \to \infty$), the total damping in the system fades ($\zeta_1 + \zeta_2 = 0$), and in such conditions, the hunting motion cannot be naturally attenuated. To solve this problem, additional damping can be introduced into the system, by employing yaw dampers [17].
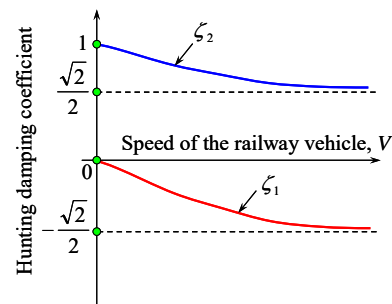

Fig. 5 Variation of the hunting damping coefficients versus the travelling speed of the railway vehicle, in the case of two vibration modes, one showing negative damping (lower red line), and the other showing positive damping (upper blue line)

VI. CONCLUSIONS

In this paper, one paid attention to dynamical aspects of the

World Academy of Science, Engineering and Technology
International Journal of Aerospace and Mechanical Engineering
Vol:12, No:1, 2018

hunting motion associated to the wheel axle of bullet trains. A generalized model that accounts for the inertial effects on the motion of the wheel axle was suggested. Based on the derived analytical expressions for the damping coefficients and damped natural frequency, one clarified the influence of the train speed, wheel conicity, dimensionless mass of the wheel axle, ratio of the creep coefficients, and, ratio of the track span to the yawing diameter, on these dynamic parameters.

Three main conclusions can be inferred from the performed analysis, as follows:

1) Natural frequency of geometrical hunting vibration mode, linearly increases against the velocity, and tends to infinity at very high running speeds of the railway vehicle. On the other hand, the damped natural frequency, associated to dynamical (inertial) hunting motion, nonlinearly increases versus the traveling speeds, tending to a finite value, when the train is running at very high velocities.

2) Geometrical hunting vibration mode occurs as undamped, and this result disagrees with the experimentally observed hunting of the actual railway carriages. On the other hand, damping ratios, related to the dynamical hunting motion, monotonically decrease at augmentation of the speed, and this agrees with the results observed during travelling tests of the railway vehicles.

3) In the absence of creep, and at very high travelling speeds of the railway vehicle, the total damping in the system fades, and in such conditions the hunting motion cannot be naturally attenuated. To solve this problem, additional damping can be introduced into the system, by employing yaw dampers.

REFERENCES

[1] S. Iwnicki, *Handbook of Railway Vehicle Dynamics*. New York: CRC Press, Taylor & Francis, 2006, pp. 21–38.
[2] A.H. Wickens, *Fundamentals of Rail Vehicle Dynamics*. New York: Swets & Zeitlinger Publishers, 2003, pp. 101–123.
[3] H. Sakai, "A Consideration to Hunting of Wheel Set," *Proceedings of JSME TRANSLOG*, 1101, pp. 1–10, 2016 (in Japanese).
[4] U. Olofsson, and R. Lewis, *Tribology of the Wheel-Rail Contact*. New York: Taylor & Francis, 2012, pp. 121–141.
[5] A. Kapoor, D.I. Fletcher, F. Schmid, K.J. Sawley, and M. Ishida, *Tribology of Rail Transport*. New York: CRC Press, 2001, pp. 161–202.
[6] D.J. Inman, and R.J. Singh, *Engineering Vibration*. New York: Prentice Hall, 2001
[7] H. Benaroya, and M.L. Nagurka, *Mechanical Vibration: Analysis, Uncertainties, and Control*. London: CRC Press, 3rd ed., 2010
[8] F.W. Carter, "On the Action of a Locomotive Driving Wheel," *Proceeding of the Royal Society London*, A112, pp. 151–157, 1926.
[9] T. Matsudaira, N. Matsui, S. Arai, and K. Yokose, "Problems on Hunting of Railway Vehicle on Test Stand," *Journal of Engineering for Industry*, 91(3), pp. 879–885, 1969.
[10] J.J. Kalker, "Wheel-Rail Rolling Contact Theory," *Wear*, 144, pp. 243–261, 1991.
[11] D. Yamamoto, "Study on the Running Vibration Characteristics of Railway Vehicle. 1st Report: Estimation of Creep Coefficient between Actual Wheel and Rail," *Journal of System Design and Dynamics*, 4(6), pp. 823–836, 2010.
[12] H. Sakamoto, and M. Yamamoto, "Effect on Nonlinear Creep Force on Railway Truck Dynamics," *Transactions of JSME*, 52(473), pp. 302–309, 1986 (in Japanese).
[13] K. Yokose, M. Igarashi, and J. Takayanagi, "Basic Investigation on the Hunting Motion of the Railway Truck by Considering the Nonlinear Characteristics of the Creep Force," *Transactions of JSME*, 51(466), pp. 1198–1208, 1985 (in Japanese).
[14] B. Suciu, "Frictional Effects on the Dynamics of a Truncated Double-Cone Gravitational Motor," *International Journal of Mechanical, Aerospace, Industrial, Mechatronic and Manufacturing Engineering*, 11(1), pp. 28–38, 2017.
[15] A.H. Wickens, "The Dynamic Stability of Railway Vehicle Wheelsets and Bogies having Profiled Wheels," *International Journal of Solids and Structures*, 1(3), pp. 319–341, 1965.
[16] M. Smith, "Train Suspension System," *Patent No. US 9403543*, pp. 1–13, 2016.
[17] B. Suciu, and R. Kinoshita, "Investigation on the Bogie Pseudo-Hunting Motion of a Reduced-Scale Model Railway Vehicle Running on Double-Curved Rails," *International Journal of Mechanical, Aerospace, Industrial, Mechatronic and Manufacturing Engineering*, 11(1), pp. 39–46, 2017.

Barenten Suciu was born on July 9, 1967. He received Dr. Eng. Degrees in the field of Mech. Eng. from the Polytechnic University of Bucharest, in 1997, and from the Kobe University, in 2003. He is working as Professor at the Department of Intelligent Mech. Eng., Fukuoka Institute of Technology. He is also entrusted with the function of Director of the Electronics Research Institute, affiliated to the Fukuoka Institute of Technology. He is member of JSME and JSAE. His major field of study is the tribological and dynamical design of various machine elements.